HST NICMOS MAPPING OF ASTEROID 4 VESTA. Jian-Yang Li, Shantanu Naidu, and Lucy A. McFadden. University of Maryland at College Park (jyli@astro.umd.edu).

Introduction: Vesta is the largest intact basaltic asteroid with a differentiated interior. It therefore carries a lot of information about the accretion and formation of terrestrial planets [1]. Intensive observations from the ground and from the space have been conducted to characterize this asteroid and to study its surface mineralogy, mainly from its characteristic pyroxene bands in the 1-μm and the 2-μm regions. Binzel et al. [2] obtained the first high-resolution surface maps of Vesta in 1994, primarily on the northern hemisphere, in the visible wavelengths (0.44 μm, 0.67 μm, 0.95 μm, and 1.02 μm) using Hubble Space Telescope (HST) Wide Field Camera for Surveys 2 (WFPC2). Since then, many other observations have been carried out to map the mineralogical composition of Vesta, including the maps focusing on the southern hemisphere obtained with the same instruments and filters on HST in 2007 [3,4]. However, since all these maps only cover the visible wavelengths, which do not include the whole 1-μm absorption band, and do not include any coverage for the 2-μm band, the mineralogical interpretation of those maps are limited.

During the 1997 opposition of Vesta, HST Near Infrared Camera and Multi-Object Spectrometer (NICMOS) obtained images in the near infrared (NIR), from ~0.95 μm to 2.37 μm, providing a complete coverage of the 2-μm band, and the long-wave side of the 1-μm band. The NICMOS images were acquired from both NIC1 and NIC2 cameras, with pixel scales 47 and 71 km/pixel on and Vesta, respectively, and phase angle of 6º. With a complete rotational coverage, these images can be used to make similar maps as generated from WFPC2 in the visible wavelengths, and provide combined analysis to better interpret the surface mineralogy of Vesta. These data are all archived in HST online database (MAST).

Data Analysis: We performed similar processing for NICMOS images as previously done by [3,4]. Specifically, for all images, we calculated the scattering geometry of the pixels inside Vesta's disk, using the shape model of Vesta [5]. The scattering geometry was then used to fit a limb-darkening model to the disk of Vesta in each wavelength with Hapke's model [6] and Minnaert's model [7]. We then use the model to remove the limb-darkening, and project the disk of Vesta onto a cylindrical longitude-latitude coordinate. The coordinate frame we used was defined with the shape model [4], with the dark feature Olbers on the prime meridian. All the projections are then combined to make the final maps. The final maps were smoothed by 10º to match the pixel scale of NICMOS during the observations.

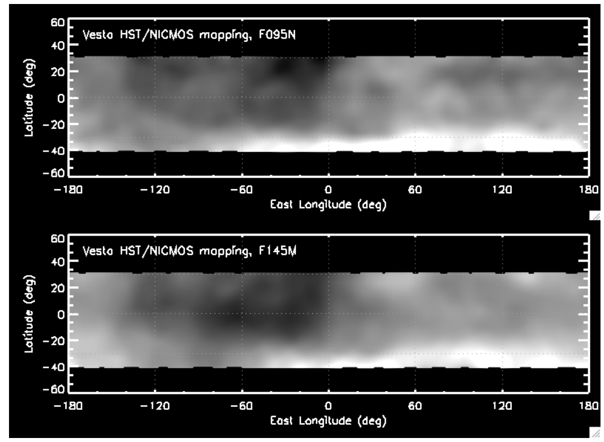

Fig. 1. The reflectance maps of Vesta in 0.95 μm (upper) and 1.45 μm (lower), constructed from HST/NICMOS images taken in 1997. The gray scale is linear from -15% to +15% relative to the average in the respective wavelength.

Preliminary maps in two wavelengths in 0.95 μm and 1.45 μm are shown in Fig. 1.

The map in 0.95 μm is similar to that reported by [2,3,4] at similar wavelength, with all the major features visible. Overall the eastern hemisphere of Vesta is brighter than the western hemisphere. The dark area near the prime meridian towards the west, interpreted by [2,3,4] as eucrite-rich area, shows up as the darkest areas in the 0.95-μm map. Near the bottom edge of the map, where it is close to the rim of the south-pole crater, the reflectance is high in 0.95-μm map. Whether this is real on Vesta, or due to different bandpassees of the NICMOS F095N filter and WFPC2 F953N filter, or it is an artifact generated during mapping process requires further investigation.

The 1.45-μm map is also consistent with the 0.95-μm map and other maps in the visible wavelengths. Again, the bright limb warrants further investigation.

The maps from other wavelengths are still in production by the time this abstract is prepared. Specifically, since the relatively large point spread function (PSF) in the NIR wavelengths, the limb-darkening of Vesta is probably substantially modified by the PSF, more significantly for longer wavelengths towards the 2-μm range. Therefore the apparent limb-darkening cannot be well modeled by light scattering models [6,7]. We are utilizing deconvolution to restore the degraded spatial resolution due to PSF, and recover the true limb-darkening of Vesta. Also, since the cadence of those images is not as dense as the images in the visible wavelengths, the final maps are expected to have slightly lower quality than visible maps.

With the wavelength coverage of NICMOS images completing the 1-µm band and including 2-µm band, we plan to finally combine these maps in the NIR with the visible maps, to characterize the band parameters for both bands. The mineralogical variations on the surface of Vesta will be interpreted based on the new maps. This work will have significant impact on the planning and final data analysis and interpretation of Dawn mission, which is scheduled to arrive at Vesta for a rendezvous in 2011 [8].

Conclusions: We constructed the maps of Vesta in the NIR wavelengths using HST/NICMOS data obtained in 1997 and archived in HST database. These maps cover wavelength from 0.95 µm to 2.37 µm. The new maps in two wavelengths are consistent with the previous maps in the visible wavelengths for the main brightness features. We will continue the mapping effort for the images in all filters. The final maps will be combined with the visible maps to construct color ratio maps, in order to extract the band parameters to characterize both the 1-µm and 2-µm bands. We will present the maps from more wavelengths in the IR, as well as the corresponding color ratio maps, and the compositional/mineralogical interpretations in the meeting.

References: [1] Keil, K. (2002) Asteroid II, pp 573-584. [2] Binzel, R.P. et al. (1997) *Icarus* 128, 95-103. [3] Li et al. (2009) Submitted to *Icarus*. [4] Li et al (2007) XXXIX LPSC (#1391). [5] Thomas et al. (1997) *Icarus* 128, 88-94. [6] Hapke, B. (1997) Theory of Reflectance and Emittance Specctroscopy. [7] Minnaert, M. (1941) *Astrophys. J.* 93, 403-410. [8] Russell, C.T. et al. (2007) *Earth Moon Planets* 101, 65-91.